JTTEE5 18:292–296
DOI: 10.1007/s11666-009-9297-2
1059-9630/$19.00

Evaluating Bending Strength of Plasma Sprayed Al_2O_3 Coatings

Zhijian Yin, Shunyan Tao, Xiaming Zhou, and Chuanxian Ding

(Submitted November 12, 2008; in revised form December 15, 2008)

The bending strength of plasma sprayed Al_2O_3 coatings was evaluated using three-point bending tests. The measured strength data sets were statistically analyzed by employing Weibull distribution. It was found that the bending strength values of coatings show obvious anisotropic behavior. Additionally, the bending strength values measured by loading parallel to the spraying direction are lower than those antiparallel to the spraying direction, and larger variability was realized for the former. This may be related mainly to the distribution of residual stress and microstructural defects within coatings.

Keywords Al_2O_3, bending strength, plasma spray, residual stress, Weibull plot

1. Introduction

Ceramic coatings produced by thermal spray techniques have been extensively used for a range of industrial applications to confer antiwear properties and erosion resistance (Ref 1-3). In such applications, the coatings experience intense mechanical loads, and, hence, for the prediction of appropriate operating conditions and service lifetime it is very useful to explore their mechanical response, which is related to mechanical properties such as hardness, elastic modulus, and strength of coatings.

It is well known that the deposit is built up by successive impingement of the liquid or partially melted droplets onto substrates in thermal spray (Ref 4, 5). These process characteristics determine the special lamellar microstructure of thermal sprayed coatings consisting of flat platelike lamellae, weak interface between splats, interlamella pores, and vertical cracks (intralamella cracks), which in turn affect the mechanical behavior of coatings. In past decades, numerous works have been reported with respect to the microhardness and elastic modulus of thermal sprayed ceramic coatings (Ref 6-10). It has been revealed that the microhardness measured on the cross section of plasma sprayed ceramic coatings by indentation technique is always larger than that while on the top surface, indicative of obvious anisotropy (Ref 6). Lin (Ref 7) and Leigh et al. (Ref 8) have extensively studied how the microhardness of thermal sprayed yttria-stabilized zirconia (YSZ) coatings varies with regard to the measurement direction and applied load. A recent study focusing on the variability and distribution of microhardness within plasma sprayed alumina coatings has pointed out that the microhardness shows certain variability and obvious dependence on the indenter location within through-thickness direction due to the special lamellar structure and microstructural defects such as pores and microcracks (Ref 9). In our previous work, it was pointed out that the elastic modulus of plasma sprayed Cr_3C_2-NiCr coatings showed much more variability than its Knoop hardness and high dependence on the testing conditions whether the major diagonal of Knoop indentation is parallel or perpendicular to the interlamellar boundaries within coatings (Ref 10). As far as the strength of thermal sprayed coatings was concerned, it generally refers to the adhesion and bending strength. In contrast to the microhardness and elastic modulus, coating strength attracts less attention, especially for the bending strength. To our knowledge, few studies have been done to investigate the relationship between bending strength of coating and its microstructural characteristics, as well as the fracture mechanics of coating sample used for bending tests.

In the current study, an Al_2O_3 coating, as an example of typical thermal sprayed ceramic deposits, was air plasma sprayed, and its bending strength was characterized by three-point bending tests under different conditions. Furthermore, the measured data sets were then statistically analyzed to estimate their reliability and variability and preliminarily discussed in terms of the microstructural characteristics and residual stress distribution within the coatings.

2. Experimental Procedures

The Metco A-2000 air plasma spraying system equipped with an F4-MB plasma torch (Sulzer Metco AG, Wohlen, Switzerland) was used to deposit coatings. Commercially available fused and crushed Al_2O_3 powders were used as feedstock and fed by a Twin-System 10-C

Zhijian Yin, Shunyan Tao, Xiaming Zhou, and **Chuanxian Ding**, The Key Laboratory of Inorganic Coatings, Shanghai Institute of Ceramics, Chinese Academy of Sciences, Shanghai 200050, P.R. China; and **Zhijian Yin**, Graduate School of the Chinese Academy of Sciences, Beijing 100039, China. Contact e-mails: shunyantao@mail.sic.ac.cn, zhijian_yin@yahoo. com.cn.

(Plasma-Technik AG, Wohlen, Switzerland). Primary and auxiliary plasma gases were Ar and H_2. The former was also used to act as a powder carrier gas. Detailed spraying parameters can be found in our publication (Ref 11). As-received powders show irregular morphology and contain pure αAl_2O_3 phase. The size distribution of starting powders is mainly in the range of 10 to 45 μm, with a medium size, (D50), of 19.3 μm. To obtain the free-standing samples used in this work, coatings with thicknesses of 3.5 to 5 mm were deposited onto an aluminum substrate and then were removed from the substrate. During spraying, the back of the substrate was cooled using circulating water, while the coating surface was cooled by compressed air.

Three-point bending tests (Instron 5566, Instron Company, USA) of the freestanding Al_2O_3 coatings specimens (3 by 4 by 36 mm) were conducted with a crosshead speed of 0.5 mm/min and a span length of 30 mm to obtain the bending strength. In order to more comprehensively evaluate the bending strength and its relationship with the coating characteristics, two machining modes for the preparation of coating specimens and three testing directions were applied, as shown in Fig. 1. Thickness of the freestanding coating sample, controlled by deposition time, used for machining mode ''a'' is smaller than that used for the model ''b,'' which means the freestanding coatings used for both models consistently suffered surface and substrate grinding of 0.05 to 0.3 mm, determined by completing grinding required. BS_1, BS_2, and BS_3, respectively, comprised 15 sets of experimental data, which correspondingly represent the bending strength values measured while the loading direction is parallel, antiparallel, and perpendicular to the spraying direction. Additionally, the measured data sets were analyzed by Weibull distribution in the two-parameter form, which is based on ''the weakest link hypothesis'' and has been found to be suitable for describing the mechanical properties of a variety of thermal sprayed coatings (Ref 9, 12).

3. Results and Discussion

Figure 2 shows the Weibull plots of the bending strength (BS) of plasma sprayed Al_2O_3 coatings measured under different loading directions, as shown in Fig. 1. All Weibull plots were approximate patterns of linearity, suggesting that the BS data sets significantly followed the Weibull distribution. Furthermore, from the statistics analysis results for all BS data sets summarized in Table 1, it can be seen that the smallest correlation coefficient (R) between the measured points and the regressed line was 0.969. This value was much larger than the critical correlation coefficient of 0.641, which is employed for a statistical test to assess whether a data set with a sample size of 15 significantly follows a regressed line under a confidence level of 0.99 (Ref 13).

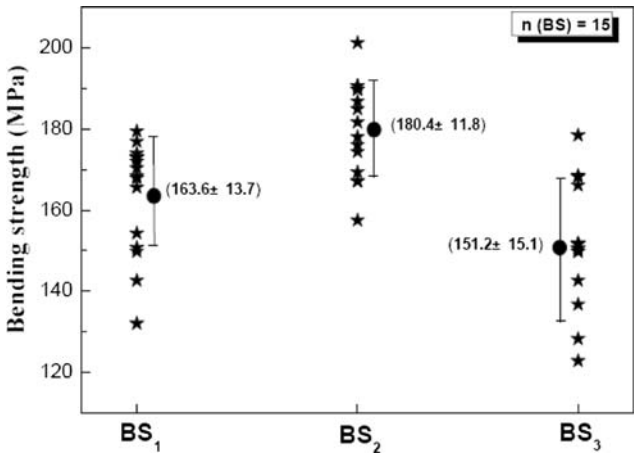

Fig. 2 Comparison of bending strength values of alumina coatings under different loading directions

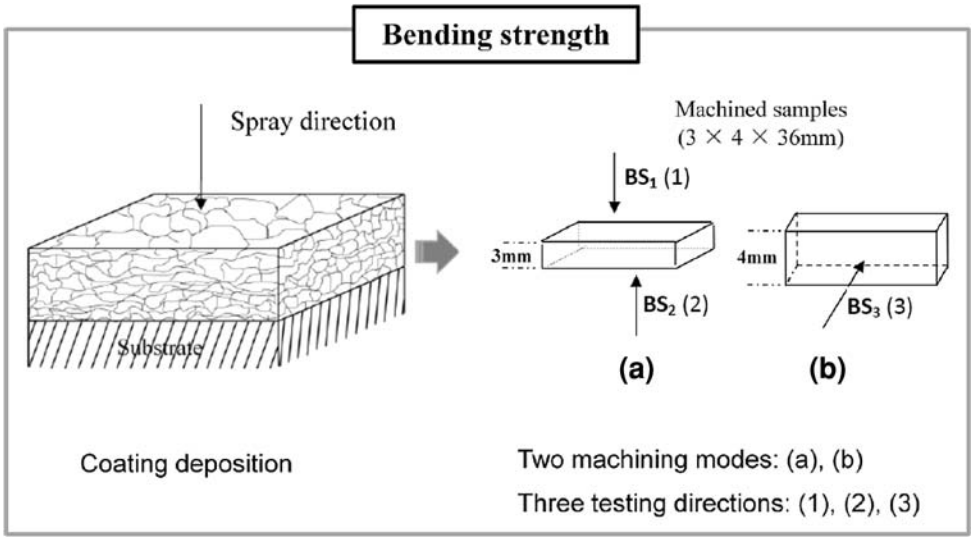

Fig. 1 Machining modes and testing direction for the characterization of bending strength of plasma sprayed coatings

Table 1 The statistical analysis results of bending strength (BS) of plasma sprayed Al_2O_3 coatings measured by loading parallel (BS_1), antiparallel (BS_2), and perpendicular (BS_3) to the spraying direction

Denotations	Average BS, MPa	Correlation coefficient, R	Weibull modulus, m	Standard deviation, MPa	Variation coefficient, V_c
BS_1	163.6	0.969	11.7	13.7	0.0837
BS_2	180.4	0.986	15.8	11.8	0.0654
BS_3	151.2	0.969	10.1	15.1	0.0999

BS_1, BS_2, and BS_3 are illustrated in Fig. 1

As illustrated in Fig. 3 and Table 1, it can be concluded that the bending strength values of the coating exhibit obvious anisotropic behavior: bending strength values measured by loading parallel or antiparallel to the spraying direction (BS_1, BS_2) larger than that while loading perpendicular to the spraying direction (BS_3). This may be attributed to the intrinsic microstructure anisotropy of plasma sprayed coatings formed by successive overlaying of molten or semimolten droplets (Ref 14, 15). Compared to BS_1 and BS_2, the BS_3 data present larger variability reflected by a lower Weibull modulus (m) of 10.1 and a larger variation coefficient (V_c) of 0.0999. Corresponding to a higher Weibull modulus and smaller variation coefficient, the data set studied becomes less variable (Ref 7, 10). If further analysis were conducted, it could be concluded that the BS_1 is lower than BS_2, and larger variability was realized for the former.

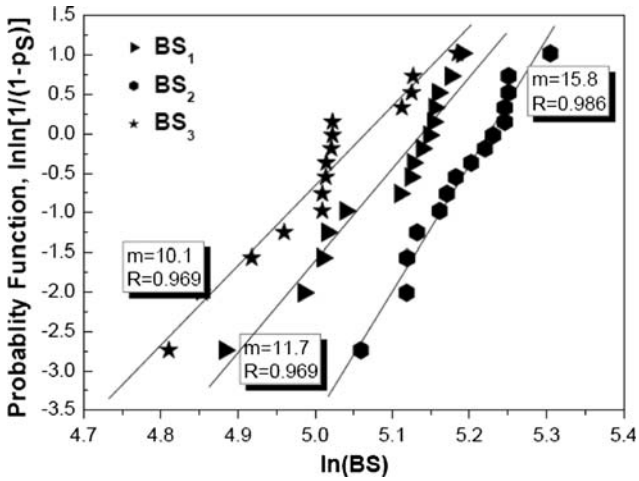

Fig. 3 Weibull plots of bending strength values for alumina coatings, where P_s is the probability of survival, m is the Weibull modulus, and R is the correlation coefficient

Prior to investigating the discrepancy between BS_1 and BS_2, it is significant and necessary to analyze the bending stress distribution and fracture mechanism for the coating sample under the three-point bending test. It is generally accepted that the compressive strength of a ceramic material is much larger than its tensile strength, even up to 10 times (Ref 16). Therefore, from the viewpoint of fracture analysis, the regions concentrated by tensile stress where crack propagation and even fracture easily occur require the preferential consideration. Figure 4 gives a schematic view of the three-point bending test, the bending stress property (tensile or compressive), and its distribution within coating sample. According to the theory of material mechanics (Ref 17), in the case of three-point bending test, the bending stress and its maximum can be formulated as (Fig. 4):

$$\sigma = \frac{My}{I_z} \quad \text{(Eq 1)}$$

$$\sigma_{max} = \frac{My_{max}}{I_z} = \frac{M}{I_z/y_{max}} = \frac{M}{W_z} \quad \text{(Eq 2)}$$

where σ is the bending stress (tensile or compressive); M is the bending torque, which is related to the value of bending load and sample dimension; y is the distance from the middle cross section through the loading direction; I_z is inertia torque indicating integrated effects of the shape and dimension as for the middle cross section; and W_z is the bending interface coefficient. Based on the previous discussion, for the coating sample the weak region, where maximum tensile stress concentrated while testing and the crack propagation and eventual fracture easily occurred, is near the surface opposite to the loading face, as seen in Fig. 4. Hence, the discrepancy between BS_1 and BS_2 can

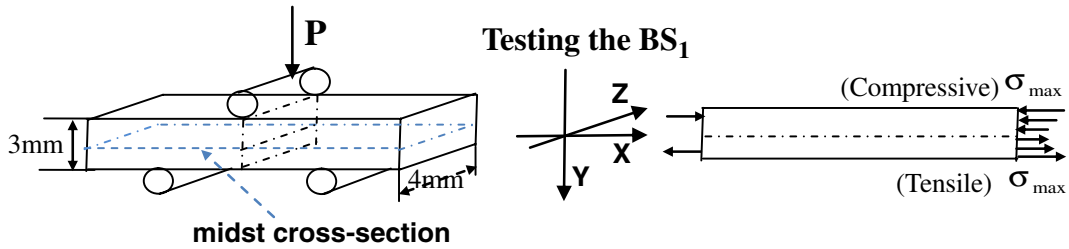

Fig. 4 Fracture analysis and stress distribution for the coating samples under three-point bending tests while loading parallel to the spraying direction (testing BS_1 as an example, P is applied load)

be preliminarily speculated to arise mainly from the distribution of microstructural defects including pores and microcracks and residual stress within plasma sprayed ceramic coatings, though requiring more experimental and theoretical analysis.

Considerable efforts have been made in recent years to understand and predict the residual stresses that develop during the deposition of thermally sprayed coatings (Ref 18, 19). Residual stresses in sprayed coatings arise from two main sources: ''quenching stress'' and ''thermal stress,'' which, respectively, are generated as the rapid quenching of molten droplets upon impact onto the substrate with restricted contraction and when cooling the completed deposit and substrate couple from deposition to ambient temperature. A single residual stress value means the stress state at a given depth below the free surface and can be tensile or compressive, depending on the different proportion of quenching and thermal stress. From the results reported by Matejicek et al. (Ref 20), residual stress of coatings, sprayed using ceramic or metal materials with lower thermal expansivity than that of the substrate material such as the aluminum used in this work, is less and even may change from tensile to compressive with an increase in coating thickness. Accordingly, though not providing experimental results of residual stress in the present study, residual stress-state differences in regions near the coating surface (weak region for achieving BS_2) or substrate surface (weak region for achieving BS_1) to some extent account for the difference between BS_1 and BS_2.

On the other hand, references in literature propose that the droplets suffer with changed cooling rate, spreading and flattening while impinging onto the substrate or previously deposited splats (Ref 21, 22). At the initial stage, the molten droplets with certain velocity and temperature impact on the cool substrate and solidify rapidly with limited spreading and flattening as a result of the high cooling rate (even up to 10^6 to 10^7 K/s, Ref 23, 24), leading to pores, microcracks, and weak interface between splats. During spraying, the droplets encounter the previously deposited splats and experience relatively sufficient spreading and good overlaying by virtue of the decreased cooling rate. This may be similar to the spraying onto the substrate with increased surface temperature by heat treatment. Safai and Herman (Ref 22) and Li (Ref 25) have pointed out that within-through coating thickness direction, the microstructural defects including pores and microcracks more easily distributed in the regions near the substrate surface. So, the distribution of microstructural defects within plasma sprayed ceramic coatings may be another significant factor resulting in the lower average value and larger variability of the bending strength measured by loading parallel to spraying direction (BS_1) compared with BS_2.

4. Conclusions

In summary, the bending strength of plasma sprayed Al_2O_3 coatings was evaluated and the measured strength data sets were statistically analyzed. It was found that the bending strength of coatings exhibits obvious anisotropic behavior. Furthermore, the bending strength values measured by loading parallel to the spraying direction (BS_1) are lower than that obtained while loading antiparallel to the spraying direction (BS_2). The former also shows larger variability. Based on the fact that during the bending test, the crack propagation and eventual fracture easily occur near the surface opposite to the loading surface where maximum tensile stresses concentrate, the discrepancy between BS_1 and BS_2 may mainly be attributed to the distribution of residual stress and microstructural defects within the coatings, meanwhile requiring more experimental and theoretical work.

Acknowledgments

The financial support of the key project of Shanghai Science and Technology Commission, Grant No. 075211017-3 is gratefully acknowledged. The authors would like to express their thanks to Ms. Zhenglan Lu for strength tests.

References

1. R. Westergard, L.C. Erickson, N. Axen, H.M. Hawthorne, and S. Hogmark, The Erosion and Abrasion Characteristics of Alumina Coatings Plasma Sprayed under Different Spraying Conditions, *Tribol. Int.*, 1998, **31**, p 271-279
2. L. Dubourg, R.S. Lima, and C. Moreau, Properties of Alumina-titania Coatings Prepared by Laser-Assisted Air Plasma Spraying, *Surf. Coat. Technol.*, 2007, **201**, p 6278-6284
3. Z.J. Yin, S.Y. Tao, and X.M. Zhou, Tribological Properties of Plasma Sprayed Al/Al_2O_3 Composite Coating, *Wear*, 2007, **263**, p 1430-1437
4. R. McPherson, On the Formation of Thermally Sprayed Alumina Coatings, *J. Mater. Sci.*, 1980, **15**, p 3141-3149
5. R.C. Dykhuizen, Review of Impact and Solidification of Molten Thermal Spray Droplets, *J. Therm. Spray Technol.*, 1994, **3**, p 351-361
6. R.S. Lima, A. Kucuk, and C.C. Berndt, Evaluation of Microhardness and Elastic Modulus of Thermally Sprayed Nanostructured Zirconia Coatings, *Surf. Coat. Technol.*, 2001, **135**, p 166-172
7. C.K. Lin and C.C. Berndt, Statistical Analysis of Microhardness Variations in Thermal Spray Coatings, *J. Mater. Sci.*, 1995, **30**, p 111-117
8. S.H. Leigh and C.C. Berndt, Evaluation of Off-Angle Thermal Spray, *Surf. Coat. Technol.*, 1997, **89**, p 213-224
9. Z.J. Yin, S.Y. Tao, X.M. Zhou, and C.X. Ding, Evaluating Microhardness of Plasma Sprayed Al_2O_3 Coating Using Vickers Indentation Technique, *J. Phys. D: Appl. Phys.*, 2007, **40**, p 7090-7096
10. J.F. Li and C.X. Ding, Determining Microhardness and Elastic Modulus of Plasma-Sprayed Cr_3C_2-NiCr Coatings Using Knoop Indentation Testing, *Surf. Coat. Technol.*, 2001, **135**, p 229-237

11. Z.J. Yin, S.Y. Tao, X.M. Zhou, and C.X. Ding, Particle In-Flight Behavior and Its Influence on the Microstructure and Mechanical Properties of Plasma-Sprayed Al_2O_3 Coatings, *J. Eur. Ceram. Soc.*, 2008, **28**, p 1143-1148
12. R.S. Lima and B.R. Marple, High Weibull Modulus HVOF Titania Coatings, *J. Therm. Spray Technol.*, 2003, **12**(2), p 240-249
13. R.E. Walpole and R.H. Myers, 2nd ed., Macmillan, New York, 1978
14. R. McPherson, The Relationship between the Mechanism of Formation, Microstructure and Properties of Plasma Sprayed Coatings, *Thin Solid Films*, 1981, **83**, p 297-310
15. A. Kulkarni, Z. Wang, T. Nakamura, S. Sampath, A. Goland, H. Herman, J. Allen, J. Ilavsky, G. Long, J. Frahm, and R.W. Steinbrech, Comprehensive Microstructural Characterization and Predictive Property Modeling of Plasma-Sprayed Zirconia Coatings, *Acta Mater.*, 2001, **51**, p 2457-2475
16. W.D. Kingery, H.K. Bowen, and D.R. Uhlmann, John Wiley & Sons, New York, 1976
17. K.P. Arges and A.E. Palmer, Eds., *Mechanics of Materials*, McGraw-Hill, New York, 1963
18. I. Kraus, N. Ganev, G. Gosmanova, H.D. Tietz, L. Pfeiffer, and S. Bohm, Residual Stress Measurement in Alumina Coatings, *Mater. Sci. Eng. A*, 1995, **199**, p L15-L17
19. Z.H. Gan, H.W. Ng, and A. Devasenapathi, Deposition-Induced Residual Stresses in Plasma-Sprayed Coatings, *Surf. Coat. Technol.*, 2004, **187**, p 307-319
20. J. Matejicek, S. Sampath, and J. Dubsky, X-ray Residual Stress Measurement in Metallic and Ceramic Plasma Sprayed Coating, *J. Therm. Spray Technol.*, 1998, **7**, p 489-496
21. R.C. Ruhl, Cooling Rates in Splat Cooling, *Mater. Sci. Eng. A*, 1968, **1**, p 313-320
22. S. Safai and H. Herman, Microstructural Investigation of Plasma-Sprayed Aluminium Coatings, *Thin Solid Films*, 1977, **45**, p 295-307
23. R. McPherson, A Review of Microstructure and Properties of Plasma Sprayed Ceramic Coatings, *Surf. Coat. Technol.*, 1989, **39-40**, p 173-181
24. A.J. Allen, G.G. Long, H. Boukari, J. Ilavsky, A. Kulkarni, S. Sampath, H. Herman, and A.N. Gland, Microstructural Characterization Studies to Relate the Properties of Thermal Sprayed Coatings to Feedstock and Spray Conditions, *Surf. Coat. Technol.*, 2001, **146-147**, p 544-552
25. J.F. Li, ''Study on Properties of Plasma Sprayed Cr_3C_2-NiCr Coatings,'' Ph.D. dissertation, Shanghai Institute of Ceramics, Chinese Academy of Sciences, 1999